

ADDITIVELY MANUFACTURED Ti2Mo FOR BIOMEDICAL APPLICATIONS: SURFACE ENGINEERING AND CORROSION PROPERTIES

Julian P. Zander¹, Stephan Lederer¹, Wolfram Fürbeth¹

¹ DEHEMA Research Institute, Frankfurt am Main, GER.

Additive manufacturing allows the fast production of small and complex parts with minimum waste for biomedical applications made of titanium alloys. However, the cytotoxicity of certain elements being widely used in these alloys has become a concern, initiating the development of new alloys avoiding their use as alloying elements. In this publication, surface engineering techniques like blasting and plasma electrolytic polishing have been applied to a new Ti2Mo alloy obtained by Selective Laser Melting (SLM) in order to enhance its surface properties. First aim of such surface engineering processes is to develop standardized surfaces for additively manufactured parts, comparable to conventionally produced parts. Residual stresses that arise due to the additive manufacturing process are examined as well as their potential impact on the mechanical and corrosion properties of the alloys. Via suitable heat treatment residual stresses can be lowered and adjusted. Additionally, the corrosion properties are determined using potentiodynamic polarization and tribocorrosion testing.

Keywords: Titanium alloy, additive manufacturing, SLM, surface engineering, corrosion properties, residual stress analysis.

1. Introduction

Among commonly used metals in the biomedical field, titanium (Ti) alloys possess favourable mechanical properties, biocompatibility, and corrosion resistance, making them an ideal choice for the fabrication of medical implants [1-2]. One of the most commonly used titanium alloy for biomedical implants is Ti6Al4V [2]. However, this alloy contains aluminium and vanadium, both cytotoxic elements that can potentially cause adverse reactions in the human body [3]. Hence, in the biomedical field the demand for new titanium alloys, which are cytotoxic-free as well as suitable for AM processing has been increasing. The titanium-molybdenum alloy Ti2Mo is a promising candidate for these purposes, offering an optimal combination of mechanical strength and biocompatibility [4].

Additive manufacturing (AM) has rapidly evolved into a major technological breakthrough in the medical industry, offering unlimited possibilities to produce implants fast and with less waste [5]. Selective Laser Melting (SLM), one of the most widespread AM techniques, is a powder bed fusion (PBF) technique that uses a high-intensity laser beam to selectively melt and solidify metallic powder layer by layer. The microstructure of the printed metal parts varies with the applied processing parameters, such as laser power density and scanning velocity, which significantly influence the mechanical and physical properties of the final product. SLM can develop complex-shaped, small structures with tight tolerances, resulting in implants that minimize the risk of post-operative complications [8-9].

The mechanical properties of SLM-manufactured Ti2Mo are superior to Ti6Al4V and cp-Ti, with a yield strength of 1006 MPa, ultimate tensile strength of 1016 MPa, and an elongation at break of

17 % [4], making it an excellent choice for load-bearing applications.

This study focuses on the surface engineering of AM Titanium alloys, in specific Ti2Mo, to generate smooth surfaces, which can be a good basis for coatings and functional structuring. Blasting with alumina removes residual particles from the AM parts and guarantees a uniformly rough surface, even for complex structures. With plasma electrolytic polishing (PEP) the micro roughness is minimized, so that the surface is smoothed [10-11]. Moreover, residual stresses are determined non-destructively by XRD and the $\sin^2\psi$ -method [12-13] in the "As Received" (AsRe), as well as in the annealed, blasted and plasma polished condition. Since the alloy Ti2Mo has been developed for biomedical applications, corrosion tests, like potentiodynamic polarization and tribocorrosion, are carried out in simulated body fluid at body temperature (37 °C).

2. Materials and Methods

2.1. Additive Manufacturing and sample preparation

Samples are additively manufactured by the Selective Laser Melting (SLM) process. Using Design of Experiments (DoE), the parameters of the process were optimized, to generate dense parts. The standard sample size was 20×15×4 mm (w×h×d) after the support structure had been removed. For the AM process, cp-Ti grade 2 and Ti2Mo (Ti 0.44O 0.08C 0.50Fe 2.00Mo) [4] powder was used. As a comparison, conventionally produced (cast) samples with the same compositions were tested. All samples were cleaned ultrasonically in ethanol and then dried with compressed air. Cleaning steps were carried out after every surface treatment. In order to lower residual stresses and transform the alpha-martensitic into an α or $\alpha+\beta$ microstructure, the AM samples were annealed for 90 minutes using an argon atmosphere in a

tube furnace at 900 °C and/or 700 °C followed by furnace cooling.

2.2. Surface engineering

2.2.1. Blasting

Samples were blasted in the blasting machine “Sigg TR60” at 3 bar compressed air. As a blasting material high-class corundum grit with a particle size distribution of 63-109 μm (according to the manufacturer) was used. Samples were blasted until a uniform surface in colour forms, at least 30 s for each side.

2.2.2. Plasma electrolytic polishing (PEP)

The surface of the AM parts was polished at a voltage of 300 V using an ITECH AC/DC power supply (IT7809-350-90). The current density was set to about 0.1 A/cm². With a heating plate the electrolyte temperature was set to 85 °C. During the PEP process the temperature rises up to 96 °C. The aqueous electrolyte consisted of NaF (1.5 %–3.0 %) and NH₄Cl (1.5 %–3.0 %) and was stirred during the process. The influence of the process time was tested between 5 to 10 minutes. Parameters were determined using a ‘Design of Experiments’ (DoE) approach targeting a minimum surface roughness (Ra).

2.3. Corrosion investigations

2.3.1. Potentiodynamic polarization

Potentiodynamic polarization tests were realized in simulated body fluids (Hanks’ solution) at 37 °C (body temperature). Temperature was set inside a heating chamber. In total, four cells equipped with a conventional three electrode setup and a volume of 200 ml each were used. The electrolyte was stirred at 400 rpm. Samples were countered against the cell opening (exhibiting an area of 0.28 cm² to the electrolyte) and connected as the working-electrode (WE) with a brass screw. Like the WE, the reference- (RE, calomel +245 mV) and counter-electrode (AE, Platinum 3-5 cm²) were connected to the OrigaFlex potentiostat. Data was analysed with the OrigaMaster5 software. Each test sequence involved a measurement of the open circuit potential (OCP) for at least 20 h followed by potentiodynamic polarization from -200 mV to +3500 mV vs. OCP.

2.3.2. Tribocorrosion

Tribocorrosion tests were realized in simulated body fluid (Hanks’ Solution) at 37 °C in a self-constructed cell (three electrode setup). The exposed sample area (WE) was 3.5 cm². Temperature was set with a flow system connected to a thermostat (Lauda ECO E4 Gold). Electrodes were connected to the OrigaFlex potentiostat. Data was analysed with the OrigaMaster5

Software. Open circuit potential (OCP, at least 20 h) and polarization resistance measurements (-20 mV to +20 mV against OCP) were performed in this setup. Tribometry tests were implemented using a Nanovea TRB (T-16-0148) pin on disc setup. The wear track of 5 mm (transversal friction) was rubbed with an alumina ball (\varnothing 6 mm) at 1 Hz frequency for a sliding distance of 40 m.

2.4. Materials characterization

2.4.1. X-ray diffraction

For phase analysis and to determine residual stresses, XRD (Bruker D8 Advance with a Cu-Cathode) was used. Measurement parameters were set with the Diffrac Commander software. For the phase analysis, 2 θ angles ranged from 30° to 90° (coupled 2 θ / θ). Data was analyzed by the Diffrac EVA software. Residual stresses were measured with the sin² ψ -method at 2 θ =139.8° ((*hkl*)=213). As a calibration for the new Ti₂Mo alloy, a stress-free sample was produced by annealing at 700 °C for 90 minutes in argon atmosphere, to determine d_0 . The reflex shift was measured from 2 θ =137.5° to 142.5° at nine different ψ -angles (sin² ψ from (-0.4) to (+0.4), step size 0.1) and three ϕ -angles (0°, 45° and 90°, 0° corresponding to build-up direction). ψ -angles were set with the offset/coupled 2 θ setting. For all measurements a fixed sample illumination of 10×5 mm was used. A z-scan prior each measurement ensured the exact height. Data was analysed with the Leptos7 software.

2.4.2. SEM

Surface images of the additively manufactured samples were captured using a Hitachi SU1000 – FlexSEM 1000II. For topographic information SE- and for material contrast BSE-mode was used at magnifications ranging from ×100 to ×5000. Phase-ratio was analysed with the software “ImageJ”.

2.4.3. Roughness

Roughness was measured by a tactile contour measuring station (MarSurf XR 1, model CT 120, equipped with a stylus BFW A 10-45-2/90, amplitude \pm 250 μm). For each sample three positions (left, middle, right) with a test track of 4 mm were measured and analysed with the MarWin software (V. 10.00-21.1) according to ISO 21920.

3. Results and discussion

3.1. Surface engineering

Figure 1 shows a comparison of the XRD patterns of SLM-produced cpTi (as received) and Ti₂Mo (as received and annealed) from 2 θ =38° to 41°.

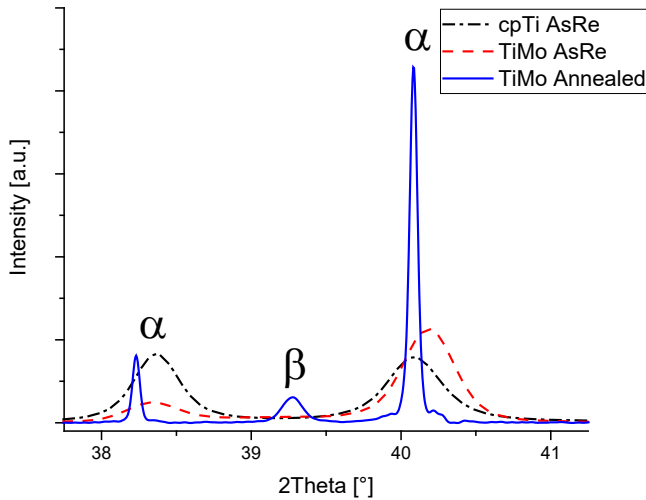


Figure 1 XRD pattern: Comparison of AM cpTi - as received vs. AM Ti2Mo - as received and annealed at $T = 900\text{ }^{\circ}\text{C}$, 90 min.

Through the high temperatures and fast cooling rates of the selective laser melting process, the Ti2Mo alloy solidifies in an alpha martensitic state. Therefore, no beta-phase is seen in the as received state, for both cpTi and Ti2Mo alloys. After annealing at $T=900\text{ }^{\circ}\text{C}$ for 90 minutes, a titanium beta phase forms because of the beta stabilization effect of Molybdenum [14].

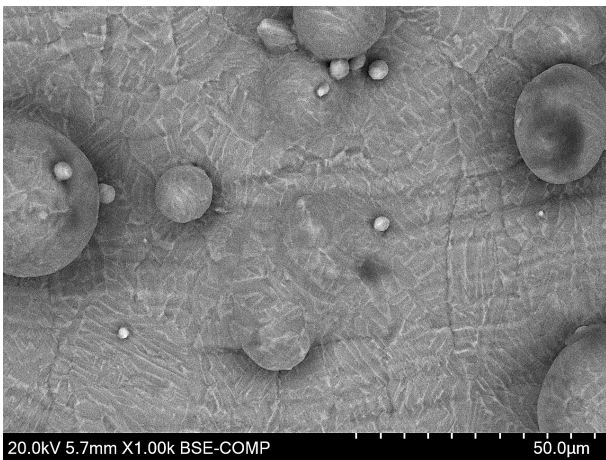


Figure 2 SEM - BSE picture, x1000 magnification. Surface and phases of AM Ti2Mo - as received, annealed at $900\text{ }^{\circ}\text{C}$ for 90 min.

In Figure 2 the $\alpha+\beta$ microstructure is represented in BSE mode by dark (α -Ti) and light (β -Ti) areas. Moreover, the surface of the additively manufactured Ti2Mo-alloy is shown in the as received state, after annealing at $900\text{ }^{\circ}\text{C}$ for 90 minutes. There is no homogeneous or even surface, due to the laser tracks and sintered spherical particles as a result of the laser melting process.

To guarantee a homogeneous and smooth surface, in the first step the samples were blasted using a high-class corundum with a small particle size

distribution ($63\text{--}106\text{ }\mu\text{m}$) and a sharp form of the blasting material, as presented in Figure 3.

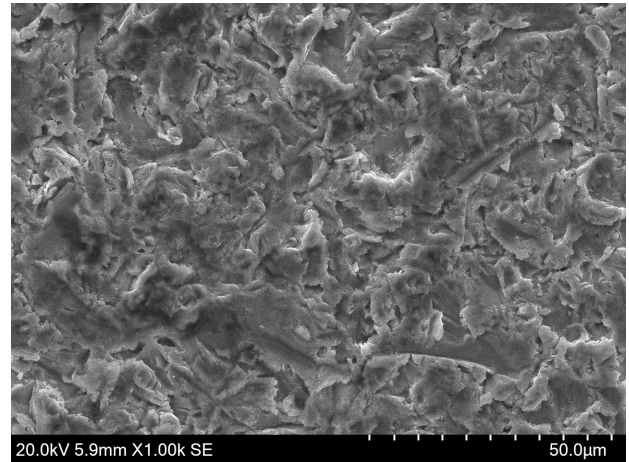


Figure 3 SEM - SE picture, surface of AM Ti2Mo - blasted with high class corundum grit of $63\text{--}106\text{ }\mu\text{m}$ in size, x1000 magnification.

Figure 4 shows the smoothed surface of the AM Ti2Mo after using the PEP process on blasted samples for 10 minutes at $85\text{ }^{\circ}\text{C}$ (T_{Start}).

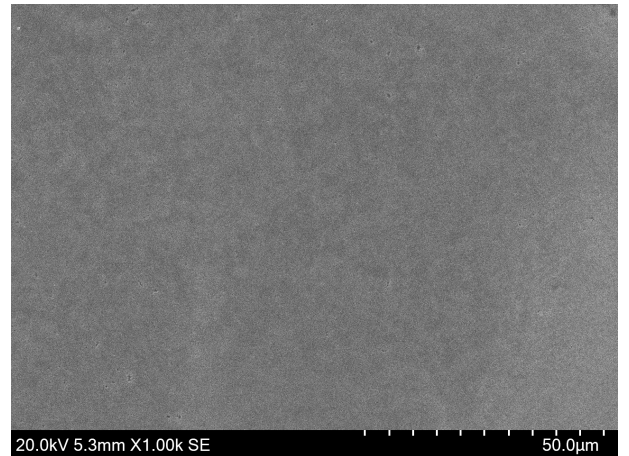


Figure 4 SEM - SE picture, surface of AM Ti2Mo - after plasma electrolytic polishing for 10 minutes at $85\text{--}96\text{ }^{\circ}\text{C}$, x1000 magnification.

During the PEP process the temperature increases up to $96\text{ }^{\circ}\text{C}$. The current density is built up until a constant value of 0.1 A/cm^2 is reached. The voltage is set to a constant value of 300 V . As the electrolyte an aqueous, low concentrated salt solution is used [16-18]. Sodium fluoride (NaF) and ammonium chloride (NH_4Cl) are dissolved in deionized water and are stirred constantly during the process. The chosen electrolyte composition, for the lowest roughness and highest optical mirror finish, is $1.5\text{ }\%$ NaF + $1.5\text{ }\%$ NH_4Cl .

Figure 5 shows the obtained average roughness (R_a , R_z) and waviness (W_a , W_q) of blasted (black) and additionally plasma electrolytically polished (red) AM Ti2Mo samples. Roughness is correlating with process

time (the longer, the smoother) and NaF-concentration in the electrolyte. NaF-concentrations higher than 1.5 % cause pitting on the surface, which leads to higher R_a - and R_z -values. Concentrations lower than 1.5 % NaF lead to an unfinished smoothed surface. The resolution of the profilometer is at 20 nm. Values of the PEP-samples, which are below this resolution, need to be verified with an optical measurement system.

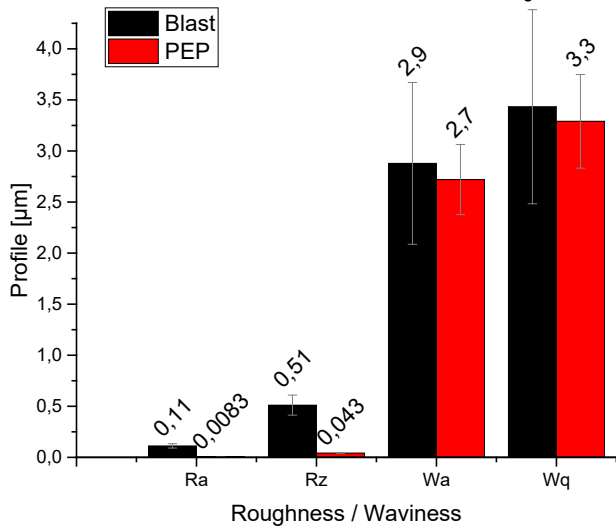


Figure 5 Mean Roughness (R_a , R_z) and Waviness (W_a , W_q) of blasted (black) and plasma electrolytically polished (red) AM Ti2Mo samples.

Since the PEP process minimizes just the micro roughness and not the overall shape of the part being polished (Figure 6), R_a and R_z values are determined in a range of 100 µm. W_a and W_q values are determined over 4 mm test length [17]. The overall waviness of the polished samples compared to the blasted ones is not changing. Only the standard deviations of the W_a and W_q values get significantly smaller by the PEP process. In contrast to the waviness, the roughness of the polished parts gets significantly smaller compared to the blasted ones. The R_a and R_z values decrease more than 90 % with very low standard deviations.

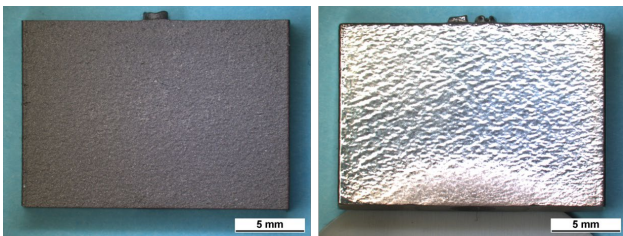


Figure 6 Left: macroscopic picture of a blasted AM Ti2Mo sample. Right: macroscopic picture of a plasma electrolytically polished sample, slightly tilted to demonstrate mirror finish and the shielding edge (side of electrical contact).

The mass loss during the PEP process depending on the process time and the electrolyte salt concentration of NH_4Cl is shown in Figure 7. The slope of the regression line presents the mean mass loss rate, which is about $8.2 \pm 0.4 \text{ mg min}^{-1}$.

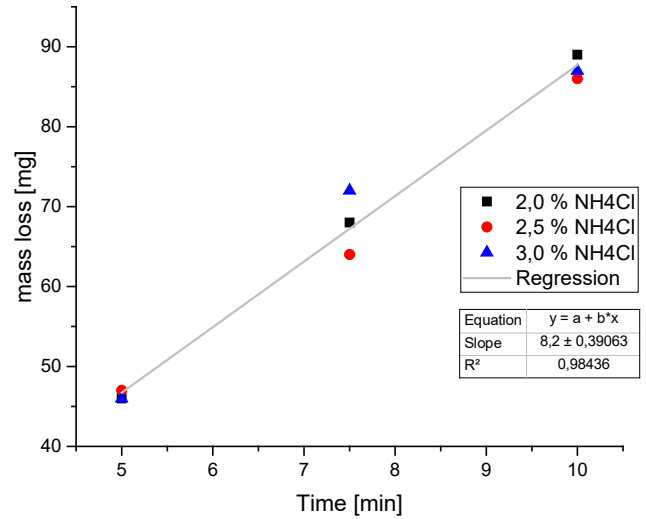


Figure 7 PEP mass loss depending on NH_4Cl concentration and process time. Mean mass loss rate about 8 mg min^{-1} .

There is no significant correlation between the mass loss and the NH_4Cl concentration of the electrolyte. Depending on the NH_4Cl concentration and process time, the shielding edge of the plasma polished samples, which is shown in Figure 6, varies. At 5 minutes and 3 % NH_4Cl the shielding edge is the largest and at 10 minutes and 1.5 % NH_4Cl the smallest.

Residual stresses, generated by the high temperatures and cooling rates of the directional AM process [19] have to be controlled in order to prevent mechanical failure. Figure 8 shows the residual stresses of a Ti2Mo sample additively manufactured by the selective laser melting process after different surface modifications. Residual stresses of the surface can be adjusted, lowered, or increased using different techniques. In the 'as received' state, the Ti2Mo samples show an anisotropic stress state, with high tensile stresses $>450 \text{ MPa}$ in built up direction (φ -angle 0°) and lowest stresses at 90° ($\sim 150 \text{ MPa}$). Positive values represent tensile and negative values compressive stresses. To ensure the accuracy of the stress values, a stress-free sample was produced previously by annealing at 700°C for 90 minutes in argon atmosphere followed by furnace cooling. The d-spacing of the stress-free sample provides a comparison for the residual stress measurement of the AM Ti2Mo alloy.

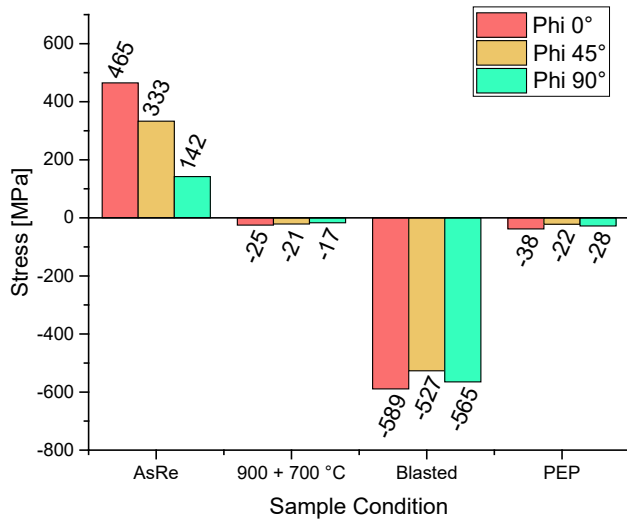


Figure 8 XRD Residual stress analysis – $\sin^2\psi$ -methode. Comparison of the stresses (φ -angle 0° , 45° , 90°) of AM Ti2Mo in four different successive conditions/preparation steps: 1. As received, 2. Annealed at $900 + 700^\circ\text{C}$, 3. blasted with high class corundum grit, 4. Plasma electrolytically polished.

After annealing at 900°C for 90 minutes in argon atmosphere (furnace cooling), a more isotropic stress state is reached. A low compressive stress is formed, which can be explained by the formation of the beta phase at 900°C resulting into a shift of the alpha titanium ($(h\ k\ l) = 2\ 1\ 3$) reflex. Additional annealing at 700°C lowers the compressive stress slightly. After blasting with high class corundum grit at 3 bar, a high compressive stress on the surface up to $\sim 600\text{ MPa}$ is formed. Through plasma electrolytic polishing the top surface is removed and residual stresses of the bulk material, comparable to the ones after the annealing step are obtained.

3.2. Corrosion investigations

Figure 9 presents the comparison of the potentiodynamic polarization curves of conventionally produced (cast) and additively manufactured (SLM) cpTi and Ti2Mo, measured in simulated body fluid (Hanks' solution) at 37°C . All samples were blasted and cleaned before the measurement. The open circuit potential (OCP) is slightly higher for the AM samples in comparison to the conventionally produced alloy in both cases. In addition to this, the AM samples show lower current densities compared to the casted samples. The AM Ti2Mo samples show the highest resistance against polarization in simulated body fluid at 37°C . Due to the fine lamellar α -martensitic microstructures, that occur by the additive manufacturing process, passive films on the titanium samples can form faster which leads to higher corrosion resistance [21].

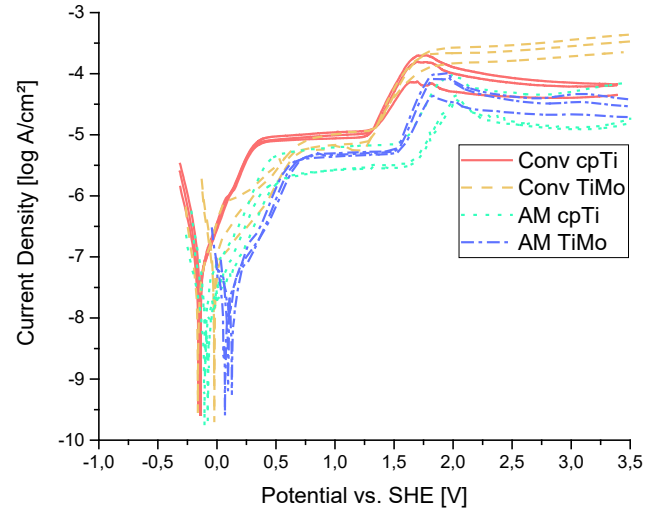


Figure 9 Potentiodynamic polarization measurements in simulated body fluid (Hanks' solution) at 37°C . Comparison between cpTi and Ti2Mo, conventionally (cast) and additively (SLM) produced.

In addition to the potentiodynamic polarization, tribocorrosion tests have been carried out for cpTi and Ti2Mo, both conventionally produced (cast) and additively manufactured (SLM). In

Figure 10 the OCP without, while (potential drop) and after (potential recovery) the friction is presented by the chronopotentiometric curves. Ti2Mo alloys show the highest starting OCP, both additively and conventionally manufactured. The AM cpTi shows a 100 mV higher starting OCP compared to the conventionally produced cpTi.

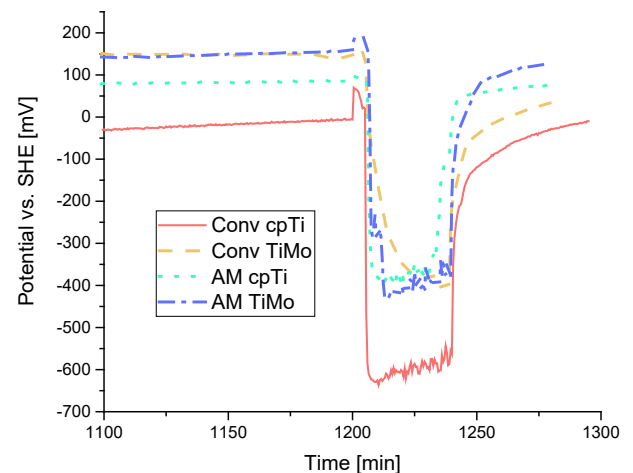


Figure 10 Electrolytic tribocorrosion measurement in simulated body fluid (Hanks' solution) at 37°C . Comparison of OCP between cpTi and Ti2Mo, conventionally (cast) and additively produced (SLM).

During friction the potential on both Ti2Mo alloys drops similarly by about 550 mV . The highest potential drop of 650 mV is observed for the cast cpTi while the lowest one of 475 mV is obtained for the SLM cpTi. The AM samples show a fast OCP recovery

reaching almost the starting value in only 30 minutes after friction has been stopped. The conventional cpTi shows a slightly lowered recovery potential compared to the AM samples while with a difference of 125 mV the cast Ti2Mo shows the lowest recovery potential.

4. Conclusion

The aim of this work with respect to surface engineering has been to design a process route towards smooth and homogeneous surfaces of additively manufactured parts, that can be compared to mechanically produced surfaces. The plasma electrolytic polishing (PEP) process in combination with previous blasting provides such a smooth surface without changing the general shape of the part. Depending on the application, like e.g. dental implant abutments or hip joint sockets, the plane surface may be used as an antibacterial one [15] or for further surface treatments such as structuring and/or coatings. Residual stresses occurring due to the AM process can be lowered and adjusted through heat treatments and surface modifications. The additively manufactured Ti2Mo alloys have proven suitable for medical implants in terms of corrosion properties since they show similar or even better corrosion resistance compared to conventionally produced cpTi and Ti2Mo.

5. Acknowledgements

The authors gratefully acknowledge the German Federal Ministry for Economic Affairs and Climate Action (BMWK) for the financial support of the project under grant number 21671 N via the German Federation of Industrial Research Associations (AiF) based on a decision of the German Bundestag. Samples were manufactured by Fabian Haase and Carsten Siemers (TU Braunschweig, Germany). Corrosion cells have been constructed by Jano Bender, Yvonne Hohmann and Heinrich Kopietz (mechanical workshop at DECHEMA Research Institute). Installation of the corrosion testing setup was supported by technician Antonio Pereira (DECHEMA Research Institute).

6. References

- Breme et al., Titanium and its Alloys for Medical Applications, *Wiley* (2003), 423-451.
- Geetha et al., Ti based biomaterials, the ultimate choice for orthopaedic implants – A review, *Progress in Materials Science, Elsevier* (2009).
- Elias et al, Biomedical Applications of Titanium and its Alloys, *JOM60*, No. 3 (2008) 46-49.
- Haase et al., Aluminum- and Vanadium-free Titanium Alloys for Medical Applications, *MATEC Web of Conferences* 321, 05008 (2020).
- Duda et al., 3D Metal Printing Technology, *ScienceDirect, Elsevier* (2016).
- Zhang et al., Powder bed fusion manufacturing of β -type titanium alloys for biomedical implant applications: A review, *Journal of Alloys and Compounds, Elsevier* (2023)
- Revilla-León et al., A Review of the Applications of Additive Manufacturing Technologies Used to Fabricate Metals in Implant Dentistry, *Journal of Prosthodontics* (2020)
- Gibson et al., Additive Manufacturing Technologies, 3rd edition, *Prosthetics and Implants, Springer* (2021) Chapter 21.3.2.
- ASTM F2792-12a: Standard terminology for additive manufacturing technologies, Geneva, Switzerland: *International Organization for Standardization* (2012).
- Zeidler et al., Plasma-Electrolytic Polishing as a Post-Processing Technology for Additively Manufactured Parts, *CIT-journal, Wiley-VCH* (2022).
- Belkin et al., Mechanism and technological opportunity of plasma electrolytic polishing of metals and alloys surfaces, *Applied Surface Science Advances, Elsevier* (2020).
- Prevéy, X-Ray Ddiffraction Residual Stress Techniques, *Metals Handbook. 10. Metals Park: American Society for Metals* (1986) 380-392.
- Luo et al., High-precision determination of residual stress of polycrystalline coatings using optimised XRD-sin 2ψ technique, *Surface & Coatings Technology, Elsevier* (2010).
- Goldberg et al., An Evaluation of B Titanium Alloys for Use in Orthodontic Appliances, *J Dent Res.* (1979)
- Seddiki et al., Evidence of antibacterial activity on titanium surfaces through nanotextures, *Applied Surface Science, Elsevier* (2014).
- Willet et al., Smoothing the surface finish of rough metal articles, EP 3 359 712 B1, *EUROPEAN PATENT SPECIFICATION* (2022)
- Nestler et al., Plasma Electrolytic Polishing – an Overview of Applied Technologies and Current Challenges to Extend the Polishable Material Range, *Science Direct, Elsevier* (2016).
- Aliakseyeu et al., Plasma Electrolyte Polishing of Titanium and Niobium Alloys in Low Concentrated Salt Solution Based Electrolyte, *MECHANIKA* (2021) Volume 27(1): 88-93
- Teixeira et al., A Review of Heat Treatments on Improving the Quality and Residual Stresses of the Ti-6Al-4V Parts Produced by Additive Manufacturing, *MDPI* (2020).
- Jáquez-Muñoz et al., Electrochemical Behavior of Titanium Alloys Using Potentiodynamic Polarization, *ECS Trans.* 101 173 (2021).
- Maleki-Ghaleh et al., Electrochemical and cellular behavior of ultrafine-grained titanium in vitro, *Materials Science and Engineering C, Elsevier* (2014).